Journal of Power Sources 195 (2010) 2355–2361

Contents lists available at ScienceDirect

Journal of Power Sources

journal homepage: www.elsevier.com/locate/jpowsour

In situ polyol-assisted synthesis of nano-SnO_2/carbon composite materials as anodes for lithium-ion batteries

Fabrice M. Courtel[a], Elena A. Baranova[b], Yaser Abu-Lebdeh[a,*], Isobel J. Davidson[a]

[a] National Research Council Canada, 1200 Montreal Road, Ottawa, Ontario K1A 0R6, Canada
[b] Department of Chemical and Biological Engineering, University of Ottawa, 161 Louis-Pasteur, Ottawa, Ontario, K1N 6N5, Canada

ARTICLE INFO

Article history:
Received 2 September 2009
Received in revised form 28 October 2009
Accepted 29 October 2009
Available online 5 November 2009

Keywords:
Composite materials
Anode
Lithium-ion battery
SnO_2
Polyol

ABSTRACT

Nano-SnO_2/carbon composite materials were synthesized *in situ* using the polyol method by oxidizing $SnCl_2{\cdot}2H_2O$ in the presence of a carbon matrix. All the as-synthesized composites consisted of SnO_2 nanoparticles (5–10 nm) uniformly embedded into the carbon matrix as evidenced by TEM. XRD confirmed the presence of nano-sized SnO_2 particles that are crystallized in a rutile structure and XPS revealed a tin oxidation state of +4. Cyclic voltammetry of the composites showed an irreversible peak at 1.4 V in the first cycle and a typical alloying/de-alloying process at 0.1–0.5 V. The best composite ("composite I", 15 wt% SnO_2) showed an improved lithium storage capacity of 370 mAh g^{-1} at 200 mA g^{-1} (~C/2) which correspond to 32% improvement and lower capacity fade compared to commercial SnO_2 (50 nm). We have also investigated the effect of the heating method and we found that the use of a microwave was beneficial in not only shortening reaction time but also in producing smaller SnO_2 particles that are also better dispersed within the carbon matrix which also resulted in higher lithium storage capacity.

1. Introduction

Lithium-ion batteries are considered as one of the best energy storage devices available for applications ranging from consumer electronic devices to electric vehicles [1]. This wide range application is due to their ability to provide a high voltage of 3.7 V, a high energy density ranging from 120 to 180 Wh kg^{-1} [2] and a good cycle life. Anode materials based on carbon are largely used because of their long cycle life, low cost and negligible volume expansion during the cycling process (insertion/extraction) [3]. However, carbon is limited to a theoretical specific capacity of 372 mAh g^{-1} and therefore alternative anode materials with higher specific capacities are much sought nowadays, especially for automotive applications. Metals and metalloids that can alloy with lithium such as Sn (993 mAh g^{-1}), Si (4200 mAh g^{-1}), Sb (660 mAh g^{-1}), Al (994 mAh g^{-1}) or their metal oxides such as SnO_2 (777 mAh g^{-1}) [4–6] are possible alternatives in this regard. Moreover, Tarascon et al. [7] demonstrated that even oxides of transition metals are also possible alternatives despite the fact that these metals do not alloy with lithium such as in Co_3O_4 (891 mAh g^{-1}) and NiO (718 mAh g^{-1}), but rather undergo a one-step reversible electrochemical conversion reaction with lithium. Despite these high capacity values, those based on Sn or SnO_2 which also have the benefit of exhibiting low reversible lithium alloying/de-alloying potential, suffer from a high volume expansion/contraction during the cycling process which results in a detrimental irreversible capacity fade [3]. Current research is focussed on the synthesis of Sn and SnO_2 nanoparticles in order to mitigate the effect of the large volume change on the cycling performance, as nanoparticles are better able to accommodate the mechanical stress experienced during volume changes. Another approach is the use of carbon as matrix substrate on which Sn or SnO_2 nanoparticles are attached. As a matrix substrate, carbon is attractive because it is inexpensive, abundant, conductive and active to lithium insertion. Chen et al. used a sol–gel method to deposit nano-SnO_2 (7.5 wt%) on the surface of carbon graphite and a capacity of 363 mAh g^{-1} was obtained. Winter et al. [8] obtained a slightly higher capacity of 380 mAh g^{-1} with a Sn (20 wt%)/carbon graphite composite made using a sodium hypophosphite as a reducing agent and sodium citrate as the complexing agent. Yang et al. [9] used carbon nanotubes as a substrate for SnO_2 nanotubes (50 wt%) prepared using a layer-by-layer technique and obtained a specific capacity of 450 mAh g^{-1}. Another important observation reported by Brousse et al. [4] is that the size of the particles plays a crucial role as smaller (nano) particles are able to better accommodate the absolute volume change than larger (micro) ones.

A well-known synthesis that is well-suited to prepare nanoparticles of metal oxides is the so-called polyol method. In brief, a high boiling point alcohol, for instance ethylene glycol (a diol), is used as a solvent, reducing agent and stabilizer. It is mixed with a tin

* Corresponding author. Tel.: +1 613 990 0347; fax: +1 613 949 4184.
E-mail address: Yaser.Abu-Lebdeh@nrc-cnrc.gc.ca (Y. Abu-Lebdeh).

0378-7753/$ – see front matter.
doi:10.1016/j.jpowsour.2009.10.086

precursor in order to precipitate SnO_2 nanoparticles. This method has already been reported by Ng et al. [10] to synthesize nanoparticles of SnO_2 which then were mixed with carbon. They obtained a stable discharge capacity of 400 mAh g^{-1} at C/4.

Herein, we report the use of the polyol method to *in situ* synthesize a composite material made of SnO_2 nanoparticles coated directly onto a carbon substrate. This was achieved by adding the carbon substrate into the reaction medium prior to the precipitation reaction. This will allow for the preparation of well-dispersed SnO_2 nanoparticles into the composites. In our study, we compared the effect of the use of a silicon oil bath (called conventional method) with another heating process that uses a scientific microwave (called microwave-assisted method). Reactions performed using a scientific microwave are generally much faster because more nucleation sites are made in a short period of time. They are also simpler and more economical than conventional heating methods [11]. Moreover, two different carbon substrates were investigated; the first is a mixture of 1/1 weight ratio of Carbon graphite and Carbon Super S (for "composite I") and the second is solely Carbon Vulcan XC-72R (for "composite II"). The first mixture has been chosen because it is usually used as an additive for the preparation of battery electrode casts [12] while Carbon Vulcan XC-72R has been selected because of its superior performance as a substrate for precious metal in the field of direct methanol fuel cells [13] mainly due to its very high surface area.

2. Materials and methods

2.1. Synthesis

The synthesis of SnO_2 was carried out using ethylene glycol (EG, HO–CH_2–CH_2–OH, Fisher). 8 g of $SnCl_2{\cdot}2H_2O$ (99.99+%, Sigma–Aldrich) were dissolved in 100 mL of EG. The solution was ultrasonicated for 5 min, stirred for 1 h and then 0.550 g of carbon powder was added. Then it was ultrasonicated again and stirred until a stable suspension was obtained. The carbon mixture used for making "composite I" was composed of 1/1 weight ratio Carbon graphite (KG, Lonza G+T, Switzerland) and Carbon Super S (Timcal graphite and Carbon, Switzerland). Carbon Vulcan XC-72R (Cabot, USA) was utilized for "composite II". The reaction medium was heated under reflux at 190–195 °C for 5 h when heated using the conventional method or 1 h when the scientific microwave was used (CEM MARS X, 600 W). The heating step was performed in air under magnetic stirring. The solution was then cooled down to room temperature overnight without stirring. Afterwards the powders were filtered using nanoporous nylon membrane filters (200 nm, Whatman), extensively washed with acetone and then dried at 80 °C for few hours before use. No further heat treatment was performed on the obtained powders.

2.2. Characterization of the composite materials

X-ray diffraction (XRD) patterns were obtained using a Cu Kα source and recorded between 15° and 85° in 2θ angle, with a step size of 0.03 and 20 s per step (Bruker D8 diffractometer). X-ray photoelectron spectroscopy (XPS) spectra were obtained using a monochromated Al X-ray source (Kratos Axis Ultra spectrometer) and were carried out using a pass energy of 40 eV for high resolution scans. CasaXPS® software was used to process the data and C 1s peak (284.7 eV) was used as a reference. The size of the SnO_2 particles was obtained by TEM (Philips CM 20). SEM pictures were made using a JSM-840A JEOL instrument. TGA analyses were performed in order to quantify the SnO_2/carbon ratio (Hi-Res TGA 2950 TA instrument). The powder was heated at 10 °C min^{-1} up to 900 °C in air. Cyclic voltammetry and cell cycling were carried out on half cells using 2325-type coin cells assembled in an argon-filled glove box. Cyclic voltammograms were recorded using a Princeton Applied Research potentiostat/galvanostat Model 263A driven by a Corrware v3.0 software. The potential of the working electrode (positive electrode) was swept at 0.1 mV s^{-1} from open-circuit potential down to 5 mV versus Li/Li^+, then swept up to 1.5 V versus Li/Li^+; afterwards cells were cycled between 1.5 V and 5 mV versus Li/Li^+. Capacity measurements were performed by galvanostatic experiments carried out on a multichannel Arbin battery cycler. The working electrode was first charged down to 5 mV versus Li/Li^+ at 200 mA g^{-1} (∼C/2) and then discharged at the same rate up to 1.5 V versus Li/Li^+. A rest step of 10 min is applied between each charge/discharge step. The mass of active material used in the calculation is the mass of the composite (i.e. carbon and SnO_2 nanoparticles).

The working electrodes were prepared as follows. (i) When the mixture of Carbon graphite and Carbon Super S was used, the active material powder was mixed with 15 wt% PVDF (Kynarflex 2800) binder dissolved in N-methyl-pyrrolidinone (NMP, Aldrich). (ii) When Carbon Vulcan was used, the active material powder

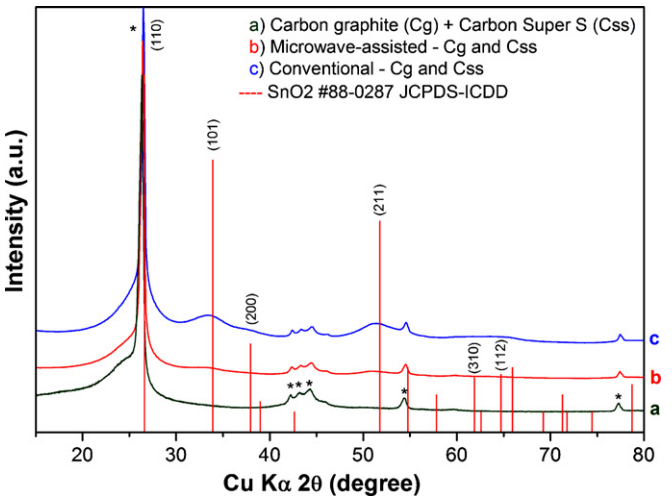

Fig. 1. X-ray diffraction patterns of the neat Carbon graphite and Carbon Super S and "composite I" obtained after drying at 80 °C. Lines at the bottom of the graph come from the 88-0287 JCPDS card of the SnO_2 rutile phase.

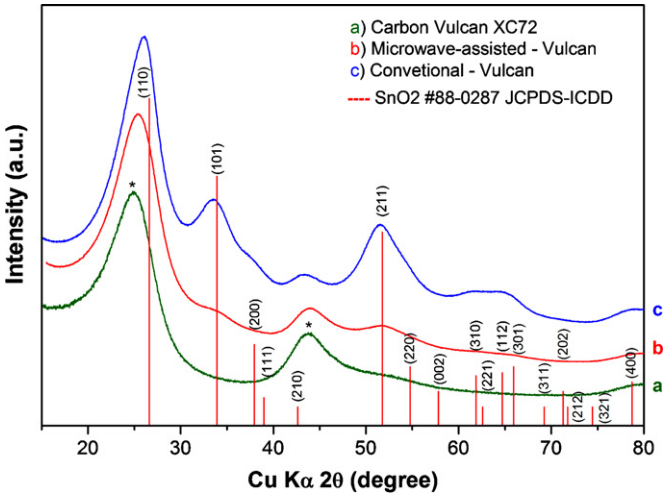

Fig. 2. X-ray diffractogram of the neat Vulcan XC-72R and "composite II" obtained after drying at 80 °C. Lines at the bottom of the graph come from the 88-0287 JCPDS card of the SnO_2 tetragonal phase.

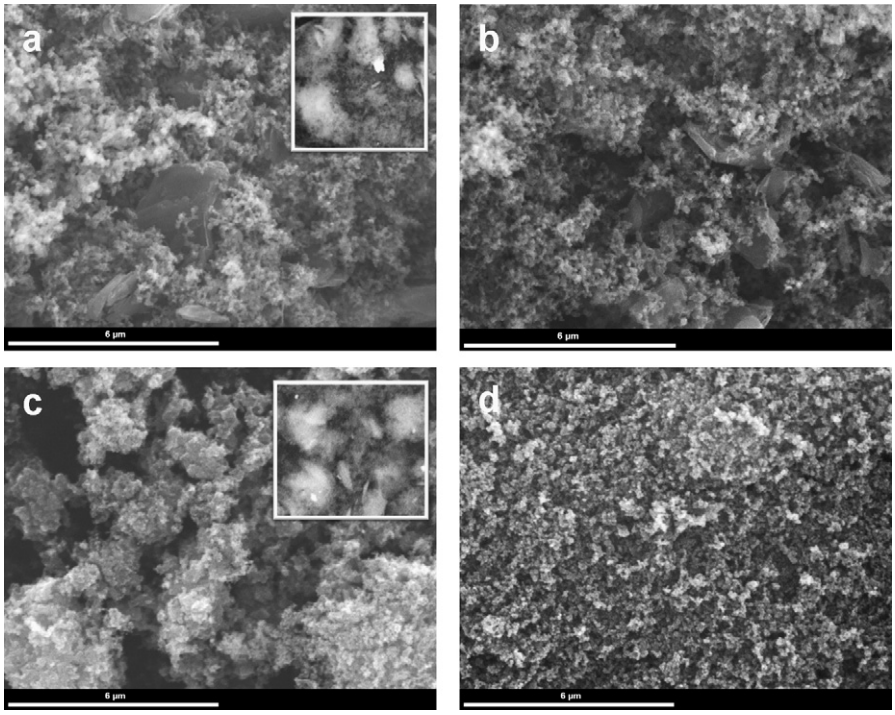

Fig. 3. SEM images of "composite I" made (a) using the conventional and (b) using the microwave-assisted method and "composite II" made (c) using the conventional and (d) using the microwave-assisted method. Inserted pictures are SEM back-scattered electrons images.

was mixed with, 5 wt% of Carbon graphite, 5 wt% of Carbon Super S and 15 wt% PVDF. (iii) A reference cell made of 75 wt% of SnO_2 nanopowder (Aldrich 50 nm), 5 wt% of Carbon graphite, 5 wt% of Carbon Super S and 15 wt% PVDF was also prepared. The electrode films were made by spreading onto a high purity copper foil current collector (cleaned using a 2.5% HCl solution in order to remove the copper oxide layer) using an automated doctor-blade and then dried overnight at 85 °C in a convection oven. Individual disk electrodes (Ø = 12.5 mm) were punched out, dried at 80 °C under vacuum overnight and then pressed under a pressure of 0.5 metric ton. A lithium metal disk (Ø = 16.5 mm) was used as a negative electrode (counter electrode and reference electrode). 70 μL of a solution of 1 M $LiPF_6$ in ethylene carbonate/dimethyl carbonate (1:1, v/v) was used as electrolyte and spread over a double layer of microporous propylene separators (Celgard 2500, 30 μm thick, Ø = 2.1 mm). The cells were assembled in an argon-filled dry glove box at room temperature.

3. Results and discussion

SnO_2/C composites were realized by combining $SnCl_2{\cdot}2H_2O$, EG and the carbon substrate under constant heating and stirring. EG is a well-known reducing agent and as explained by Bock et al. [13], in the case of Pt and Ru, the oxidation of EG is a two-step reaction. The interaction of the –OH groups with the M^{n+} ions results in the EG oxidation to 2-hydroxyethanal (HO—CH_2—CH=O) in a two-electron process and then to oxaldehyde (O=CH—CH=O) by another two-electron process. The released electrons from these oxidation reactions result in the reduction of the M^{n+} to M^0. A similar mechanism can be envisaged for the reduction of Sn^{2+} and as the reaction is completed in air, Sn^0 can be easily oxidized to SnO_2. However, as shown by Joseyphus et al. the reduction of metals such as Sn, Ni, Co, Fe, Cr or Mn using the polyol method is more sophisticated; Sn^{2+} is almost at the limit of EG reducing power [14], which explains the very low yield obtained for this reaction, being between 5 and 10%. Ng et al. proposed a different pathway [10] where $SnCl_2$ is firstly hydrolyzed to $SnOH^+$ and then oxidized to SnO_2.

Fig. 1 displays the X-ray diffractograms of the neat Carbon graphite/Carbon Super S mixture and "composite I" (nano-SnO_2, Carbon graphite and Carbon Super S) prepared using both the conventional and the microwave-assisted method. As can be seen from diffractogram (a), the basic peaks of Carbon graphite (hexagonal 2H) are observed, namely the strong (0 0 2) diffraction line at about 26° and some lower intensity lines between 40° and 47°, at 55° and 77° (they are marked with * in Fig. 1). Vertical lines represent the diffraction peaks of SnO_2 tetragonal structure (rutile) as supported by the 88-0287 JCPDS-ICDD file. The positions of the measured SnO_2 X-ray peaks also correspond well with the JCPDS-ICDD file and with the literature [15]. Nevertheless, the main SnO_2 diffraction peak is superimposed on the main Carbon graphite diffraction peak. Compared to the conventional method, the microwave-assisted method provided SnO_2 particles that have broader peaks, which indicates the formation of either smaller and/or less crystalline particles. Fig. 2 shows the X-ray patterns of the neat Carbon Vulcan XC-72R and its SnO_2 "composite II" prepared using the two heating methods. As illustrated in diffractogram (a), the basic broad peaks of Carbon Vulcan XC-72R are observed at about 25° and 44°. As observed for "composite I", the main SnO_2 diffraction peaks are superimposed on the main Carbon Vulcan diffraction peak. Once again, compared to the conventional method, the microwave-assisted synthesis provided broader X-ray peaks.

The morphology of the composites was studied by SEM and their images are shown in Fig. 3. Pictures of "composite I" (a) and (b), showed big flaky particles of Carbon graphite and smaller particles of Carbon Super S. Pictures of "composite II" (c) and (d), showed small particles of Carbon Vulcan. Fig. 4 shows TEM images of the as-prepared composites. In all cases, it is evident that the SnO_2 nanoparticles are embedded at the surface of the carbon particles in a uniformly dispersed fashion. Moreover, the powder obtained by the microwave-assisted method exhibit slightly smaller particle sizes (~5 nm) than that prepared by the conventional method (~10 nm) and also a higher degree of dispersion of the SnO_2 nanoparticles at the carbon surface. It is known that carbon is a microwave active element, as discussed by Rao at al. [11]

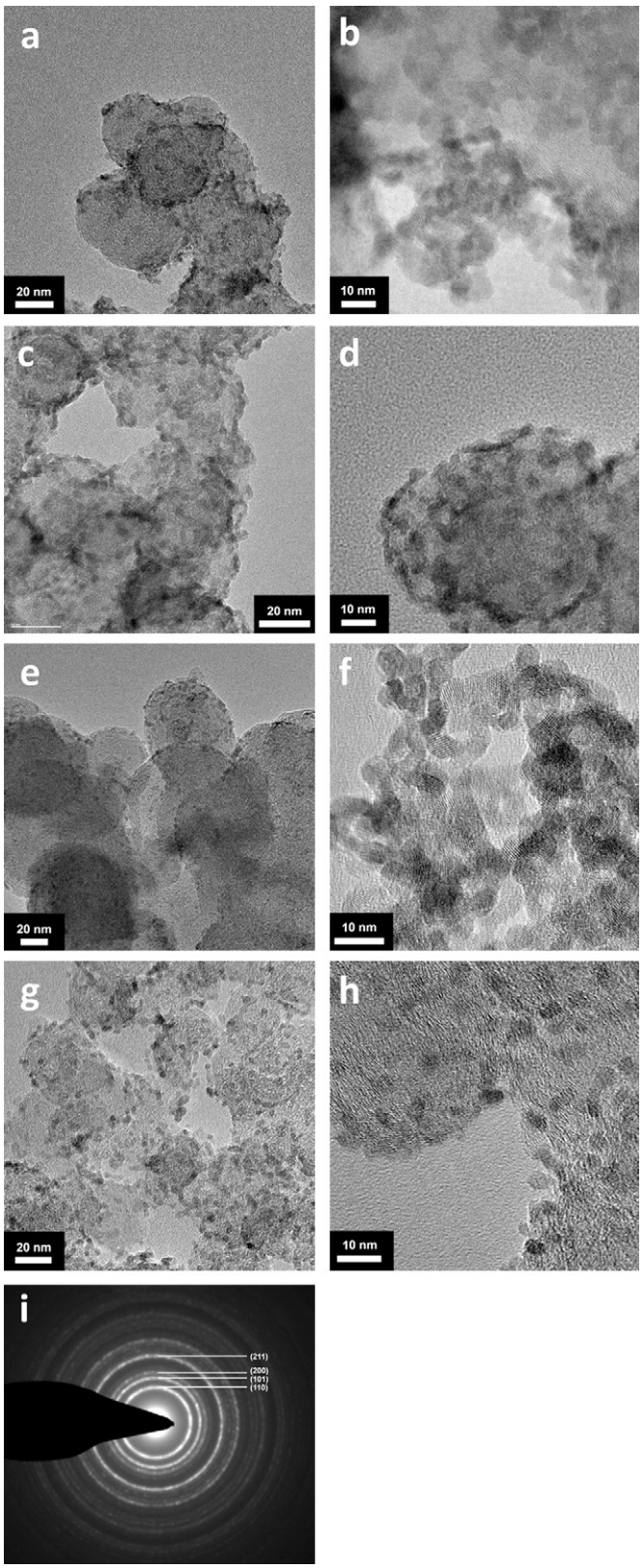

Fig. 4. TEM images of "composite I" (a and b) using the conventional and (c and d) using the microwave-assisted method and "composite II" (e and f) using the conventional and (g and h) using the microwave-assisted method. (i) An electron diffraction pattern of "composite I" synthesized by the microwave-assisted method.

Table 1
Weight percentage of SnO_2 in the bulk of the composite materials obtained by TGA and SnO_2 on the surface obtained by XPS.

SnO_2 in wt%	Conventional		Microwave-assisted	
	TGA	XPS	TGA	XPS
Composite I	24 ± 2	61.3 ± 1.0	15 ± 1	62.7 ± 0.1
Composite II	30 ± 2	41.0 ± 0.1	15 ± 2	48.8 ± 0.3

and Subramanian et al. [15]. The advantage of the *in situ* synthesis (i.e. by adding carbon at the beginning of the reaction) is that the large number of hot spots induced by the microwave might have an effect on the carbon surface properties, leading to surface modifications that enhances its interaction with SnO_2. This in turn will lead to higher SnO_2 nucleus density which results in well-dispersed SnO_2 nanoparticles at the carbon surface. Using TEM we have also obtained an electron diffraction pattern as shown in Fig. 4(i). The main diffraction lines have been assigned to (1 1 0), (1 0 1), (2 0 0) and (2 1 1) diffraction planes of the tetragonal SnO_2 phase. This assignment is in agreement with what is reported in Ref. [15] for the same material. From the ring pattern we can conclude that the powder is polycrystalline and composed of randomly oriented crystals.

XPS measurements have been done to determine the oxidation state of Sn. The Sn 3d spectra, recorded for the obtained powders, are shown in Fig. 5. As shown in Fig. 5(a), "composite I", made either by the conventional or by the microwave-assisted method, exhibit almost identical Sn 3d spectra. The right peak corresponds to the $3d_{5/2}$ level while the left one to the $3d_{3/2}$ level. The $3d_{5/2}$ peak has a binding energy of 487.2 eV. This position agrees well with the Handbook of X-ray photoelectron spectroscopy [16] and the work of Subramanian et al. [15], giving a Sn oxidation number of +4. As shown in Fig. 5(b), "composite II" exhibits a $3d_{5/2}$ peak at a slightly higher energy, at 487.6 eV. A difference of 0.4 eV is observed between the two carbon substrates that is most probably due to the fact that the C 1s level is used as a reference and set at 284.7 eV. The two carbon substrates used are different which explains the shift observed for the position of Sn $3d_{5/2}$ peaks; the same behaviour was observed for the O 1s peak.

In order to quantify the weight percentage of SnO_2, the as-synthesized composites were analyzed by TGA; the results are shown in Table 1. The conventional method provided a SnO_2 loading (weight percent of SnO_2 in the bulk of the composite) of 24% "composite I" and 30% "composite II", whereas the microwave-assisted method provided a lower loading of 15% for both composites. However, when the conventional method was used, SnO_2 aggregates were formed (100–500 nm), as observed in the SEM picture of the back-scattered electrons (inset in Fig. 3(a) and (c)). Back-scattered electrons are electrons that are reflected from the sample by elastic scattering and the intensity of their signals is related to the atomic number of the element (heavy elements in white and light elements in black). The white spots represent the SnO_2 aggregates.

XPS has been used to determine the surface loading of SnO_2 at the surface of carbon (as the SnO_2 loadings obtained by TGA correspond to the bulk of the composite material). It has been observed that the nature of carbon has an effect on the SnO_2/C ratio. As shown in Table 1, "composite I" showed a higher SnO_2 content at the surface reaching 61–62 wt% whereas "composite II" gave a lower SnO_2 content of 41 and 49 wt% for the powder prepared using the conventional and the microwave-assisted method, respectively. Our attempts to increase the bulk and the surface SnO_2 loading by increasing the precursor/carbon ratio led to the same values which means that a maximum SnO_2 loading was reached for the two carbon types used.

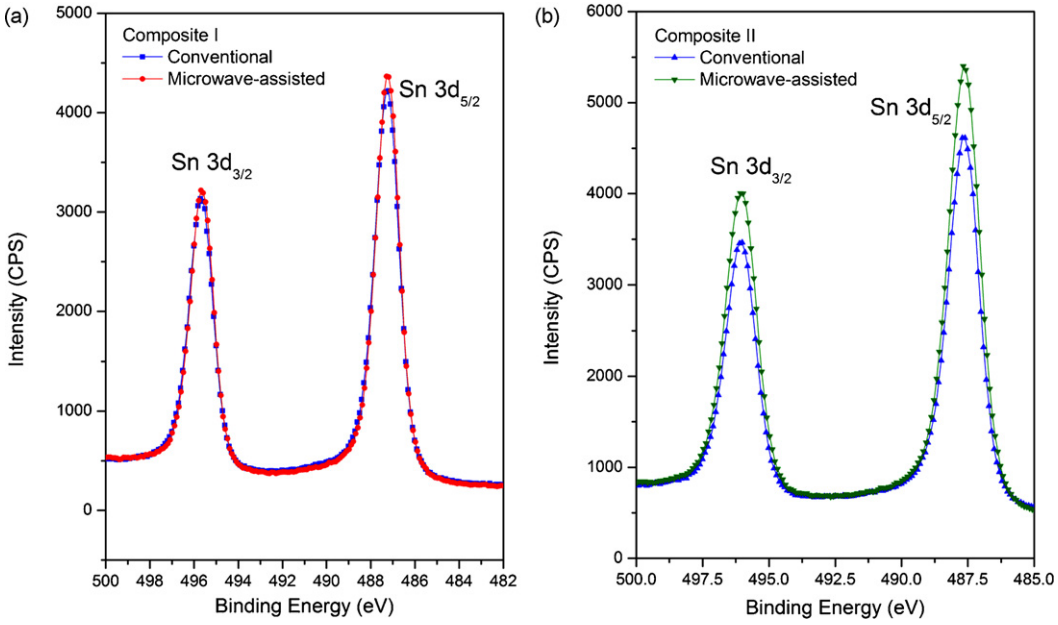

Fig. 5. XPS spectra of the Sn 3d level of "composites I and II".

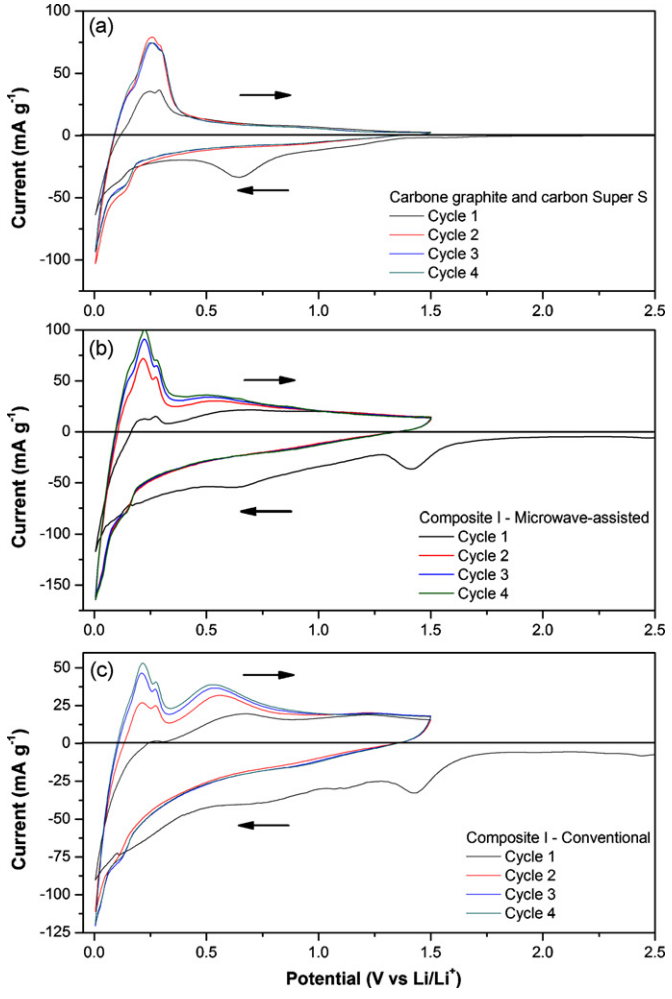

Fig. 6. Cyclic voltammetry of (a) a Carbon graphite and Carbon Super S electrode, (b) "composite I" prepared using the microwave-assisted method and (c) "composite I" prepared using the conventional method. Batteries were first cycled between OCP and 5 mV and to 1.5 V and then cycled between 1.5 V and 5 mV versus Li/Li^+.

Fig. 6 shows the cyclic voltammograms of an electrode made of the mixture of Carbon graphite/Carbon Super S (a), an electrode of "composite I" prepared using the microwave-assisted (b) and the conventional method (c). The potential range where most of the lithium insertion occurs is at about 0.1–0.01 V versus Li/Li^+ whereas the lithium extraction occurs around 0.25 V for carbon and 0.5 V for tin. In Fig. 6(a), the main cathodic peak at 0.65–0.70 V is related to the known solvent decomposition leading to the formation of a stable solid electrolyte interface (SEI) which fully disappears on the second cathodic sweep [17]. The other cathodic processes closer to 0 V correspond to lithium insertion into carbon (Li_xC_6, $x<1$). The anodic peaks between 0.2 and 0.35 V correspond to lithium extraction from Li_xC_6. "Composite I" made using the microwave-assisted method showed a first reduction process at about 1.4 V. This process has been attributed to SnO_2 reduction that usually appears at about 0.8 V [4] but as already observed by other groups [18], this positive potential shift might be attributed to the size confinement of the metal oxide nanoparticles that leads to an enhancement of the electrochemical activity at the surface. It could also be possible that the strong interaction between C and O atoms weakens the Sn–O bond, which leads to a lower energy and higher reduction potential. SnO_2 reacts with lithium in a two-step process, shown by Eqs. (1) and (2):

$$SnO_2 + 4Li^+ + 4e^- \rightarrow Sn + 2Li_2O \quad (707\,mAh\,g^{-1}) \tag{1}$$

$$Sn + xLi^+ + xe^- \leftrightarrow Li_xSn \quad (0 \le x \le 4.4,\ 993\,mAh\,g^{-1}\,Sn) \tag{2}$$

The first reaction (Eq. (1)) is totally irreversible; as evidenced by the disappearance of the peak at about 1.4 V in the second cathodic sweep [19]. The second peak at about 0.65 V is related to the formation of the SEI [17,19] and it disappears on the second cathodic sweep. As previously explained, the cathodic peak at lower potentials corresponds to the Li_xC_6 formation and the reversible formation an Li_xSn alloy ($0 \le x \le 4.4$, Eq. (2)). The first group of anodic peaks between 0.15 and 0.30 V correspond to lithium-ion extraction from Li_xC_6 and the last anodic peak at about 0.55 V was attributed to the decomposition of Li_ySn. We also observed that "composite I" prepared via the conventional method showed a similar behaviour (Fig. 6(c)).

Fig. 7 shows cyclic voltammograms of a Carbon Vulcan XC-72R electrode (a), an electrode made of "composite II" prepared via the

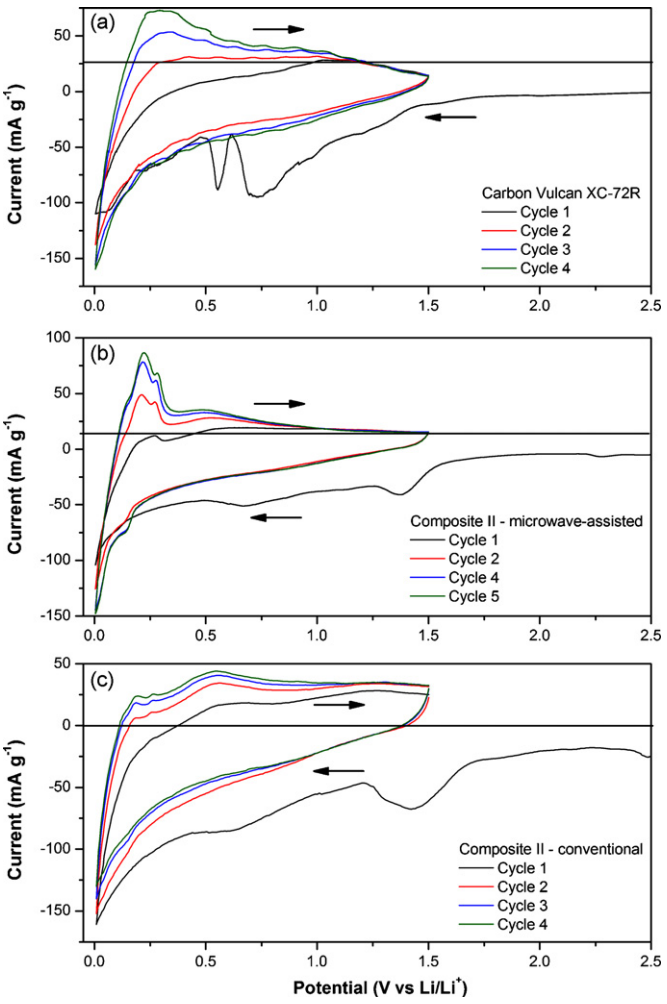

Fig. 7. Cyclic voltammetry of (a) a Carbon Vulcan XC-72R electrode, (b) "composite II" prepared using the microwave-assisted method and (c) "composite II" prepared using the conventional method. Batteries were first cycled between OCP and 5 mV and to 1.5 V and then cycled between 1.5 V and 5 mV versus Li/Li^+.

microwave-assisted (b) and the conventional method (c). The Carbon Vulcan voltammogram shows a different behaviour from the previous carbon mixture; it exhibits a first peak at 0.75 V and a second one at 0.5 V that appear only for the first cycle. They can be attributed to the formation of the SEI. "Composite II" prepared via the microwave-assisted method showed a similar behaviour to the previous composite material, a first cathodic peak at 1.4 V, corresponding to SnO_2 reduction, is observed. The second peak at about 0.7 V (related to the SEI formation) also disappears on the second cathodic sweep. The alloying and de-alloying process occured at similar potentials to "composite I" (0.1/0.5 V).

Figs. 8 and 9 show the discharge capacities as a function of cycle number for both composites. As shown in Fig. 8, the Carbon graphite/Carbon Super S mixture provided a stable capacity of 280 mAh g^{-1} at a cycling rate of 200 mA g^{-1} (~C/2). As previously explained, in the case of SnO_2, a first conversion reaction reduces SnO_2 to Sn (Eq. (1), theoretical capacity: 707 mAh g^{-1}) and then the formation of Li_xSn takes place (Eq. (2), theoretical capacity of 777 mAh g^{-1} SnO_2). The total theoretical capacity of this reaction is 1484 mAh g^{-1} SnO_2. The theoretical capacities of the composites for the first discharge and the subsequent discharges can be calculated using the composites' weight percentages obtained by the TGA measurements. The first discharge of "composite I", made using the conventional method, showed a capacity of 545 mAh g^{-1}, which represent 96% of the total theoretical capacity (569 mAh g^{-1})

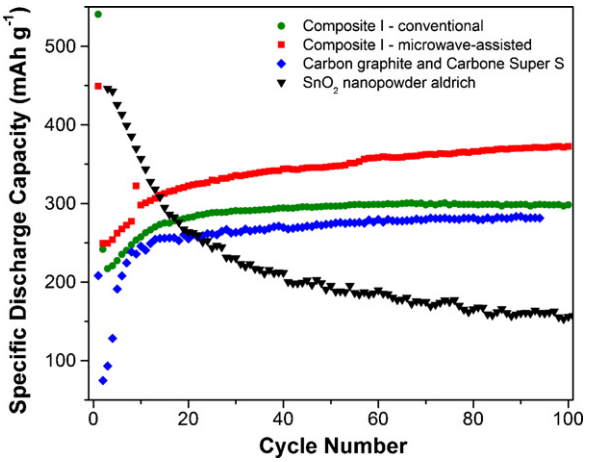

Fig. 8. Cycling behaviour of "composite I" and SnO_2 nanopowder from Aldrich (50 nm). Cells cycled between 5 mV and 1.5 V versus Li/Li^+ at a cycling rate of 200 mA g^{-1}.

whereas when prepared using the microwave it showed a first discharge capacity of 450 mAh g^{-1} which represents 98% of the theoretical capacity (460 mAh g^{-1}). After 100 cycles, the material obtained via the conventional method exhibited a stable capacity of 300 mAh g^{-1} while a capacity of 370 mAh g^{-1} was observed when made via the microwave-assisted method. Compared to neat carbon, these values represent a capacity increase of 7 and 32%, respectively, and capacity retentions of 81% and slightly over 100%, respectively. Using the conventional polyol method to synthesize neat SnO_2 nanoparticles, Ng et al. [10] managed to obtain a very stable specific capacity of 400 mAh g^{-1} after 100 cycles at a rate of 200 mA g^{-1}. However, for obtaining neat SnO_2 nanoparticles it is necessary to use acetone to partially precipitate the SnO_2 nanoparticles. The filtration and precipitation process led to a very low yield, about 5%. Using a non-precipitation method, such as a sol–gel method, Chen et al. synthesized a composite material of SnO_2 nanoparticles (7.5 wt%) and Carbon graphite. They obtained a specific capacity of 363 mAh g^{-1} after 30 cycles at a rate of C/5; this capacity value is similar to what have been obtained in the present study (15 wt%) after 100 cycles at a higher discharge rate (~C/2).

The neat Carbon Vulcan provided a lower discharge capacity of 207 mAh g^{-1} as shown in Fig. 9. The first discharge of "composite II" made using the conventional method showed a capacity

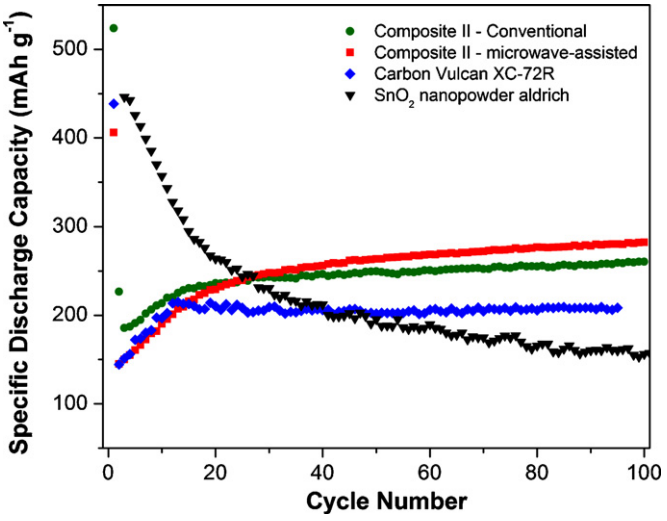

Fig. 9. Cycling behaviour of "composite II". Cells cycled between 5 mV and 1.5 V versus Li/Li^+ at a cycling rate of 200 mA g^{-1}.

of 525 mAh g^{-1} which represents 89% of the theoretical capacity (590 mAh g^{-1}). This capacity is higher than the one prepared using the microwave-assisted method (400 mAh g^{-1}) which represents 100% of the theoretical capacity (400 mAh g^{-1}). As previously observed for "composite I", after 100 cycles, "composite II" prepared using the conventional method exhibited a stable capacity of 260 mAh g^{-1} whereas a capacity of 285 mAh g^{-1} was obtained for the microwave-assisted method. Compared to neat Vulcan, these values represent a capacity increase of 25 and 37%, respectively, and capacity retentions of 69 and 97%, respectively.

The capacity values were initially low but after cycle number 10 the cells reach a stable value. This can be attributed to technical issues related to the wetability of the electrodes. Due to the homogenous distribution of SnO_2 nanoparticles at the surface of the carbon substrates, the specific discharge capacities do not fade with the cycle number, even after 100 cycles which was not the case for the SnO_2 nanopowder obtained from Aldrich (see Figs. 8 and 9). It showed a large capacity fade as shown in Fig. 8. However, composite materials prepared using the conventional method exhibit lower capacities even though the first discharge capacities are higher. This is explained by the presence of SnO_2 aggregates that become disconnected from each other and lose electrical contact which was corroborated by TGA and SEM observations.

Finally, it is worth mentioning that we attempted to make composites with MCMB (Osaka Gas, Japan) as a carbon substrate because of its known high and stable reversible capacity of about 350 mAh g^{-1} at C/12. Unfortunately, no SnO_2 phases were observed at the surface of the carbon substrate as evidenced by XRD and XPS using neither the conventional nor the microwave-assisted heating methods.

4. Conclusions

Nano-SnO_2/carbon composites were prepared via the so-called polyol method using either the conventional or the microwave-assisted heating method. The *in situ* synthesis has provided well-dispersed SnO_2 particle with a rutile phase as evidenced by XRD embedded onto carbon substrate. Overall, composite materials obtained via the microwave-assisted method have smaller particle sizes (5 nm) compared with composite materials made via the conventional method (10 nm), as verified by TEM measurements. Electrochemical testing of the composites showed a reversible lithium alloying/de-alloying process between 0.005 and 1.5 V after an expected first irreversible reaction. "Composite I" presented here provides enhanced lithium storage capacity reaching 370 mAh g^{-1} compared to the neat carbon and the neat SnO_2 electrodes, which represent a 32% improvement. Regardless of the carbon type, composites prepared using the microwave-assisted method provided an improved reversible and stable capacity.

Acknowledgements

The authors thank the Canadian Program of Energy Research and Development for the financial support, Dr. Dashan Wang for the TEM analyses, Mr. David Kingston for the XPS and SEM analyses and Dr. Christina Bock for providing the Vulcan XC-72R.

References

[1] G.-A. Nazri, G. Pistoia, Lithium Batteries: Science and Technology, Kluwer Academic Publisher, Boston/Dordrecht/New York/London, 2004.
[2] J.M. Tarascon, M. Armand, Nature 414 (2001) 359–367.
[3] M.N. Obrovac, L. Christensen, D.B. Le, J.R. Dahn, J. Electrochem. Soc. 154 (2007) A849–A855.
[4] T. Brousse, O. Crosnier, J. Santos-Peña, I. Sandu, P. Fragnaud, D.M. Schleich, in: N. Kumagai, S. Komaba (Eds.), Materials Chemistry in Lithium Batteries, Research Signpost, Kerala, 2002.
[5] H. Nara, Y. Fukuhara, A. Takai, M. Komatsu, H. Mukaibo, Y. Yamauchi, T. Momma, K. Kuroda, T. Osaka, Chem. Lett. 37 (2008) 142–143.
[6] Y.-C. Chen, J.-M. Chen, Y.-H. Huang, Y.-R. Lee, H.C. Shih, Surf. Coat. Technol. 202 (2007) 1313–1318.
[7] P. Poizot, S. Laruelle, S. Grugeon, L. Dupont, J.M. Tarascon, Nature 407 (2000) 496–499.
[8] A. Trifonova, M. Winter, J.O. Besenhard, J. Power Sources 174 (2007) 800–804.
[9] N. Du, H. Zhang, B. Chen, X. Ma, X. Huang, J. Tu, D. Yang, Mater. Res. Bull. 44 (2009) 211–215.
[10] S.H. Ng, D.I. dos Santos, S.Y. Chew, D. Wexler, J. Wang, S.X. Dou, H.K. Liu, Electrochem. Commun. 9 (2007) 915–919.
[11] K.J. Rao, B. Vaidhyanathan, M. Ganguli, P.A. Ramakrishnan, Chem. Mater. 11 (1999) 882–895.
[12] A. Abouimrane, I.J. Davidson, J. Electrochem. Soc. 154 (2007) A1031–A1034.
[13] C. Bock, C. Paquet, M. Couillard, G.A. Botton, B.R. MacDougall, J. Am. Chem. Soc. 126 (2004) 8028–8037.
[14] R.J. Joseyphus, T. Matsumoto, H. Takahashi, D. Kodama, K. Tohji, B. Jeyadevan, J. Solid State Chem. 180 (2007) 3008–3018.
[15] V. Subramanian, W.W. Burke, H. Zhu, B. Wei, J. Phys. Chem. C 112 (2008) 4550–4556.
[16] J.F. Moulder, W.F. Stickle, P.E. Sobol, K.D. Bomben, Handbook of X-ray Photoelectron Spectroscopy: A Reference Book of Standard Spectra for Identification and Interpretation of XPS Data, Perkin-Elmer Corporation, Eden Prairie, 1992.
[17] P.B. Balbuena, Y. Wang, Lithium-Ion Batteries: Solid-Electrolyte Interphase, Imperial College Press, London, 2004.
[18] J.Y. Kim, D.E. King, P.N. Kumta, G.E. Blomgren, J. Electrochem. Soc. 147 (2000) 4411–4420.
[19] Z.-Q. He, X.-H. Li, L.-Z. Xiong, X.-M. Wu, Z.-B. Xiao, M.-Y. Ma, Mater. Res. Bull. 40 (2005) 861–868.